A Length Scale Dependent Model for Stress Relaxation in Polymer Melts

Michael F. Herman

Department of Chemistry, Tulane University, New Orleans, Louisiana 70118

Received July 20, 2000; Revised Manuscript Received April 19, 2001

ABSTRACT: A model for the plateau in the relaxation modulus is presented. This model treats the relaxation on successively longer length scales. The extent of relaxation in the strain-induced excess free energy for each length scale is evaluated by minimizing the free energy through motions on that length scale, while constraining the system such that there is no relaxation on all longer length scales. The extent of relaxation is determined by the number of other chain segments in contact with a relaxing chain segment. The residual excess free energy, which remains after the relaxation on a length scale, is further reduced by the subsequent relaxation on the longer length scales. This analysis predicts that the entanglement chain length for relaxation should scale as $N_e \sim \rho^{-2} b^{-3} b_1^{-3}$, where ρ is the monomer density, b is the monomer bond length, and b_1 is the Kuhn length. Two methods for the evaluation of the time dependent relaxation modulus, which are based on this length scale dependent analysis of the relaxation, are proposed and compared.

I. Introduction

In a recent paper,[1] we have argued that the extent of relaxation in a polymer melt, following the application of a strain, varies depending on the length scale under consideration. This analysis minimizes the free energy per chain segment on a given length scale, subject to the constraint that the chain is not allowed to relax on longer length scales. Given the model employed for the length scale dependent free energy, the relaxation is nearly complete on short length scales, but the fraction of unrelaxed excess free energy grows with length scale, approaching unity for longer length scales. The extent of relaxation on each length scale is determined by the average number of chain segments in contact with a given chain segment on this length scale. The total excess free energy per monomer is obtained by summing the contributions from all length scales, and this summed excess free energy determines the plateau in the relaxation modulus.

In this paper, a more general and improved model is provided for the length scale dependence of the excess free energy. The analysis considered in the previous work[1] assumes a rather restrictive form for the dependence of the free energy on n_{chj}, the number of segments of other chains in contact with a given chain segment on the jth length scale. The analysis presented in this work begins with a completely general dependence of the length scale dependent free energy on n_{chj}. Moreover, model calculations are presented in the appendices, which provide insight into the expected functional form for the free energy at long length scales. It is also argued in this paper that the relaxation on each length scale further reduces the residual unrelaxed free energy on all shorter length scales, resulting in significantly more relaxation for short length scales than was the case in the previous treatment. Furthermore, if the length scale dependence of the residual free energy is chosen to be consistent with the long length scale form suggested by the model calculations, then the additional short length scale relaxation leads to a different scaling dependence of the entanglement chain length, N_e, on the monomer density, ρ, the monomer bond length, b, and the Kuhn length, b_1, than would be the case for the previous model.[1] In both the current and previous treatments, the length scale dependent free energy can only depend on n_{chj}, given the Gaussian coil model used to describe the chains. This results in N_e depending only on the combination of quantities $\rho^2 b^3 b_1^3$ in both treatments. This n_{chj} is also the quantity employed in packing length arguments[2] to obtain the dependence of N_e on $\rho^2 b^3 b_1^3$. However, in our length scale dependent analysis, the functional dependence of N_e on $\rho^2 b^3 b_1^3$ is determined by the manner in which the free energy depends on n_{chj}, and this leads to the different dependence of N_e on $\rho^2 b^3 b_1^3$ in the current and previous treatments. The N_e values predicted in this work are found to be in good agreement with published experimental values for several polymer systems. The entanglement chain length determines the magnitude of the plateau modulus.[3] Importantly, the free energy analysis of the relaxation presented is independent of the mechanism for the chain motion. Therefore, these results do not rest on any assumption about nature of the chain motion.

This paper is organized as follows. The analysis of the length scale dependent relaxation of the strain-induced excess free energy is presented in section II. Numerical calculations are presented in section III, which compare calculated values of N_e with published experimental results. Numerical results are also discussed, which verify the accuracy of some of the approximations made in obtaining the scaling of N_e on the monomer density, the monomer bond length, and the Kuhn length and which test the sensitivity of N_e on the form employed for the length scale dependent free energy. Calculations are also presented for the time dependent relaxation modulus. The results are discussed in section IV, and model relaxation calculations are presented in the appendices.

II. Theory of the Length Scale Dependent Relaxation

To evaluate the stress in a polymer melt, we consider the relaxation of chain segments on consecutively longer

10.1021/ma001268d CCC: $20.00
Published on Web 05/23/2001

length scales. The chain segments on each length scale contain twice as many monomers as was the case for the segments on the previous length scale. Therefore, $n_j = 2^j n_0$, where n_j is the number of monomers along the chain backbone in a chain segment on the jth length scale. The three-dimensional distance corresponding to the jth length scale scales as $l_j = 2^{1/2} l_{j-1}$, as long as the segment length is longer than the persistence length for the chain. We set n_0 to unity and l_0 is proportional to $(bb_1)^{1/2}$, where b is the monomer bond length and b_1 is the Kuhn length. In this work, the monomer bond length is defined as the average bond length along the chain backbone, and the number of monomers is taken to be the number of bonds along the backbone. In this analysis, the chains are viewed as being composed of harmonically bonded beads. In going from one length scale to the next, two beads of the chain are combined into one bead for the next length scale. The bond length for the new bead is $2^{1/2}$ times the bond length for the beads on the previous length scale.

In this work, the relaxation is considered on each length scale, subject to the constraint that there is no relaxation on the next longer length scale. The free energy associated with this length scale after relaxation is a well-defined thermodynamic quantity for this constrained system. The assumption here is that this description provides a reasonable model for the relaxation in polymer melts. There are various ways in which the relaxation of the strain-induced excess free energy associated with the jth length scale could be evaluated, subject to the constraint that the chain does not relax on the $(j + 1)^{st}$ length scale. One way would be to allow the relative position of two consecutive beads in a chain to relax, subject to the constraint that the average position of the two beads is held fixed. An alternative approach is employed in this paper. The relaxation on a given length scale is modeled by constraining the position of every other bead on this length scale to be fixed and allowing the unconstrained beads to relax. The reduction in the excess free energy per relaxing bead can then be evaluated on this length scale. The excess free energy associated with the $(j + 1)$st length scale is then evaluated in this same way, and so on. We are treating the relaxation as taking place on successive length scales by removing the constraints and allowing relaxation on one length scale, then removing the constraints and allowing relaxation on the next length scale, and so on. In a real system, this is more or less what occurs, since relaxation on longer length scales requires longer relaxation times.

The feature of the length scale dependent relaxation, which is important for the current analysis, is the dependence of the excess free energy on the number of chain segments in contact with a given chain segment on each length scale, where the excess free energy is defined as the difference between the free energy per segment in the strained system and its equilibrium value. Given that the chains are viewed as harmonically bonded beads with every other bead held fixed on each length scale and the relaxation on each length scale involves small chain segments containing a single relaxing bead, the number of segments in contact with the relaxing segment is the only quantity on which the extent of relaxation can depend for each length scale. A model calculation for the free energy of a system containing segments of two chains is presented in Appendix A. A similar model for the relaxation of one chain segment in a system containing many chain segments is presented in Appendix B.

In the one-dimensional two chain relaxation model in Appendix A, the end beads of two three-bead chain segments are held fixed, while the middle beads are allowed to move. Initially, the middle beads have an equilibrium distribution of positions, given the fixed locations of the end beads. An affine elongation strain is applied to all the beads. The free energy is evaluated for the set of configurations obtained from the affine deformation of the initial equilibrium configuration distribution. The middle beads are then allowed to relax subject to the constraint that the chains cannot cross, and the free energy is evaluated after the relaxation is complete. It is found that the relaxation reduces the free energy associated with the distribution of positions for the middle beads to a value just slightly above the initial equilibrium free energy. (This residual excess free energy does not include the extra free energy due to the strain-induced stretching of the distance between the end beads, which is associated with the next length scale.) This residual excess free energy results because the probability of one chain being on a particular side of the other chain reflects the equilibrium distribution of positions for the middle beads in the segments before the strain, which is not the same as the equilibrium distribution for the system given the strain altered positions of the end beads. The free energy expressions for this two chain model are generalized in Appendix B to the case of many three-bead chain segments with fixed end beads in contact with each other. Limiting expressions are obtained for the case of a large number of chain segments, n_{ch}, and it is argued that the residual excess free energy scales as $1/n_{ch}^2$ in this large n_{ch} limit.

The number of chain segments in contact with a given chain segment on the jth length scale, n_{chj}, depends on the number of monomers per segment, n_j. This dependence of n_{chj} on n_j can be evaluated by the following scaling argument. The volume spanned by a chain segment containing n_j monomers is proportional to $V_{chj} \sim (n_j bb_1)^{3/2}$, where $n_j bb_1$ is the mean-squared end-to-end distance for the segment. There are ρV_{chj} monomers in this volume, where ρ is the monomer density. Since each segment contains n_j monomers, the number of other chain segments in contact with any given chain segment on the jth length scale scales as $n_{chj} \sim \rho V_{chj}/n_j \sim B n_j^{1/2}$, where $B = \rho(bb_1)^{3/2}$. Because this argument rests upon the assumption that the number of chain segments in mutual contact is proportional to the number of segments in the volume defined by the segment radius of gyration cubed, it is very similar to the argument used in the packing length analysis of the scaling of the plateau modulus and entanglement length.[2]

The fraction of the initial excess free energy that is unrelaxed on the jth length scale, subject to the constraint that there is no relaxation on the $(j + 1)$st length scale, is given by

$$F_j = \Delta A_{2j}/\Delta A_{1j} \tag{1}$$

where $\Delta A_{ij} = (A_{ij} - A_{0j})$. A_{0j} is the equilibrium free energy per chain segment, A_{1j} is the poststrain free energy per segment before the relaxation, and A_{2j} is the free energy per segment after the relaxation on the jth length scale. The variable γ is the elongation ratio or the shear ratio, depending on the type of strain applied. The lowest order in $\Delta\gamma$ contributions for both ΔA_{1j} and

ΔA_{2j} are proportional to $(\Delta\gamma)^2$, where $\Delta\gamma = 1 - \gamma$ for an elongation and $\Delta\gamma = \gamma$ for a shear, since the first derivative of A with respect of γ must be zero for the equilibrium system. It is easily seen that this $(\Delta\gamma)^2$ dependence corresponds to the *linear* response of the system. The stress can be obtained by taking the derivative of the free energy per unit volume with respect to γ. The modulus is then obtain by dividing the stress by $\Delta\gamma$. Thus, the $(\Delta\gamma)^2$ terms in ΔA_{1j} and ΔA_{2j} provide a stress which is linear in $\Delta\gamma$ and a modulus which is independent of $\Delta\gamma$. This corresponds to the linear regime. F_j is also independent of γ in the linear regime. Since the resulting modulus is the second derivative of the free energy density with respect to a deformation of the system *evaluated for the equilibrium system*, it is an equilibrium averaged quantity, as it should be.

During the relaxation on the jth length scale, the middle bead of each rescaled three-bead segment relaxes, while the end beads are held fixed, and the free energy associated with the chain segments on this length scale decreases from ΔA_{1j} to $\Delta A_{2j} = F_j \Delta A_{1j}$. The relaxation on the jth length scale allows each bond on this length scale to assume a distribution of configurations, which is closer to its equilibrium configuration than was the case before the relaxation. Recall that each *bond* on the jth length scale corresponds to a three-bead, two-bond segment on the $(j - 1)$st length scale. The relaxation of the configurations of the bonds on the jth length scale toward equilibrium corresponds to the same relaxation in the distribution of end-to-end displacements for the segments on the $(j - 1)$st length scale, and this relaxation in the end-to-end displacement produces a reduction in the residual excess free energy for the $(j - 1)$st length scale, $\Delta A_{2,j-1}$.

Since both ΔA_{1j} and ΔA_{2j} are proportional to $(\Delta\gamma)^2$, ΔA_{2j} is the same free energy that would be associated with the jth length scale before relaxation, if the bonds on this length scale had had a strain applied to them corresponding to a value of $(\Delta\gamma_j)^2 = F_j(\Delta\gamma)^2$ rather than $(\Delta\gamma)^2$. To calculate the free energy on the $(j - 1)$st length scale after the relaxation on the jth length scale, we approximate the postrelaxation distribution of relative positions of the two end beads of this segment on the $(j - 1)$st length scale as that which would be produced before relaxation, if the original strain had been given by $\Delta\gamma_j$ instead of $\Delta\gamma$. Within this approximation, the excess free energy on the $(j - 1)$st length scale, which is proportional to $(\Delta\gamma)^2$ before relaxation on the jth length scale, is proportional to $(\Delta\gamma_j)^2$ after relaxation on the jth length scale. Thus, after the relaxation on the jth length scale, $\Delta A_{2,j-1}$ equals $(\Delta\gamma_j)^2/(\Delta\gamma)^2$ times its value before the relaxation on the jth length scale. Since $F_j = (\Delta\gamma_j)^2/(\Delta\gamma)^2$, the additional fractional reduction in the excess free energy on the $(j - 1)$st length scale due to the relaxation on the jth length scale is the same as the fractional reduction in the excess free energy for the jth length scale.

By the same reasoning, the additional relaxation on the $(j - 1)$st length scale accompanying the relaxation on the jth length scale produces the same fractional reduction in the residual excess free energy on the $(j - 2)$nd length scale, and so on. Thus, the relaxation of the free energy by a factor of F_j on the jth length scale produces an additional relaxation by the factor F_j on *all* shorter length scales. After relaxation has taken place on the first j length scales, the fraction of the initial stress that is unrelaxed on the lth length scale, for $l < j$, is given by

$$H_l = F_l \prod_{i=l+1}^{j} F_i = \exp[-\sum_{i=l}^{j} f_i] \tag{2}$$

where $f_i \equiv -\ln(F_i)$. The product of the F_i factors accounts for the relaxation on the lth length scale due to the relaxation on all longer length scales up to the jth. In the model calculation presented in Appendix B, it is found that $F_i \approx 1 - (C/n_{\mathrm{chi}})^2$ and $f_i \approx (C/n_{\mathrm{chi}})^2$ in the large n_{chi} limit, where C is a constant. If we assume, for the sake of example, that this expression for f_i holds for all i and that $n_{\mathrm{chi}}{}^2 = B^2 n_i = B^2 n_0 2^i$, then eq 2 gives $H_l = \exp[-2(C/B)^2/(n_0 2^l)]$ in the large j limit.

The total excess free energy *per monomer* after the relaxation is obtained by summing the remaining excess free energy per monomer on all length scales

$$\Delta a = \sum_{l=1}^{\infty} \Delta A_1 H_l / n_l \tag{3}$$

where ΔA_1 is the excess free energy per n_l monomer segment before relaxation. In this work, we are treating the chain segment on the lth length scale as a three-bead, harmonically bonded chain with the end beads fixed. In this harmonic model, the effect of the strain is the same on each length scale before relaxation, and ΔA_{l1} is independent of length scale. The subscript l has been left off ΔA_1 in eq 3 to indicate that this quantity is independent of the length scale. Since $n_l = 2^l$ and $H_l = 1$ for all l immediately after the application of the strain, eq 3 gives $\Delta a = \Delta A_1$ as the total excess free energy per monomer before relaxation. The free energy per volume is obtained by multiplying the free energy per monomer, Δa, by the monomer density, ρ. After relaxation has taken place on the first j length scales, then the H_l factors in eq 3 for $l \leq j$ are given by eq 2. The length scale dependence of the extent of relaxation in the free energy, as given by eqs 2 and 3, is the main result of this work.

There is a longest length scale in real polymer melts, for which n_j equals the number of monomers per chain, N. On the time scale of the longest relaxation time, the chain diffusion results in the disengaging of the contacts between all pairs of chains that were initially in contact. When this happens, the stress on the longest length scale completely relaxes. This results in complete relaxation on all length scales. This can be seen from eq 2, since $F_j = 0$ for the longest length scale. However, there is a range of intermediate times for long chains, where the process of relaxation on successively longer length scales produces negligible further relaxation, since the F_j's for the length scales relaxing at these times differ little from unity. The values of the H_j's, Δa, and $G(t)$ are essential converged, and they remain at this converged value until the chains disengage on the time scale of the terminal relaxation time. The value of the relaxation modulus, $G(t)$, obtained from this converged free energy before the chains disengage is the plateau modulus, G_N. This can be evaluated in the long chain limit by setting the upper limit on the product of F_i factors in eq 2 to infinity.

The scaling of the entanglement length, N_e, can be determined by approximating the summation over length scales in eq 3 as an integration and extending

the lower limit of integration to zero, based on the expectation that almost complete relaxation on short length scales gives $H_j \approx 0$ and $H_j/n_j \approx 0$ for small n_j. With these modifications, Δa takes the form

$$\Delta a \approx \frac{\Delta A_1 B^2}{\ln(2)} \int_0^\infty \mathrm{d}x \, \frac{H(x)}{x^2} \tag{4}$$

where $x = B^2\, 2^j$ and $H(x)$ is given by

$$H(x) = \exp\left[-\int_x^\infty \mathrm{d}y \, \frac{f(y)}{y \ln(2)}\right] \tag{5}$$

with y defined as $y = B^2\, 2^i$. The extension of the upper limit of integration to infinity in eqs 4 and 5 is valid in the long chain limit. Since F_j depends only on $n_{\mathrm{ch}j} \propto x^{1/2}$, given the length scale rescaling procedure employed here, f_i depends only on y and the integral in eq 5 depends only on the value of the lower limit x. Consequently, $H(x)$ only depends on x, and the integral in eq 4 is a constant, independent of the properties of the specific polymer system. The only dependence on the properties of the polymer arises through the factor of B^2 in eq 4. The entanglement length is proportional to the inverse of the fraction of the initial excess free energy that remains after the relaxation, $N_\mathrm{e} \equiv \Delta A_1/\Delta a$. Thus, according to eq 4, N_e scales as B^{-2}, giving

$$N_\mathrm{e} \sim \rho^{-2} b_1^{-3} b^{-3} \tag{6}$$

This is the same scaling as predicted in the work of Fetters et al.[2] based on the packing length concept.

The relaxation on progressively longer length scales considered in this model provides a procedure for the evaluation of the entanglement length, N_e, and, equivalently, the plateau modulus. It also has implications for the time dependent stress relaxation of a strained system. However, a calculation of the time dependent relaxation modulus, based on the length scale dependent theory of relaxation presented here, requires a prescription for associating time scales with the different relaxation length scales in the theory. The size of the relaxing chain segments on each length scale is given in the theory in terms of n, the number of monomers in the segment. The segment radius of gyration, R_g, provides a natural length scale for the n-monomer segment. The length scale for the time dependent motion of the segments is determined by the monomer mean-squared displacement, $g(t)$. We associate a time scale with each length scale by assuming that relaxation takes place for segments on all length scales for which R_g^2 is less than or equal to $g(t)$; that is, for all segments for which the length scale for the segment is less than or equal to the length scale for the motion. If the chains are approximated as Gaussian coils, then $R_\mathrm{g}^2 = nbb_1/6$. Equating R_g^2 and $g(t)$ gives $n(t) = 6g(t)/bb_1$ for the number of monomers in the largest relaxing segments as a function of time.

Given this connection between the longest relaxing length scale and the time, two procedures are compared for the evaluation of the time dependent relaxation modulus. Since the free energy is proportional to $(\Delta\gamma)^2$, we have $G(t)/G(0) = A(t)/A(0)$. The first method for evaluating the modulus, $G(t)$, uses $n_j = 6g(t_j)/bb_1$ to associate a relaxation time t_j with each relaxation length scale n_j. The contribution to the excess free energy from this length scale is assumed to decay exponentially from ΔA_{1j} to ΔA_{2j} with decay time t_j. The relaxation is evaluated by replacing the relaxed values of F_j in eq 2 with the time dependent values, $F_j(t) = \exp(-t/t_j) + F_{j\infty}[1 - \exp(-t/t_j)]$. This $F_j(t)$ decays exponentially from its unrelaxed value of unity to its relaxed value of $F_{j\infty}$. In the calculations, the long chain limit is employed, so that the upper limit on the product in eq 2 is extended to infinity. The second method considered for the evaluation of $G(t)$ employs eq 4, which treats the relaxation length scale as a continuous variable. In this approach, all length scales $n < n(t)$ are treated as having their postrelaxation value of F_j, and all length scales with $n > n(t)$ are treated as completely unrelaxed. This corresponds to replacing the upper limit on the integral in eq 5 with the finite value x_max, which corresponds to $n(t)$. [If this upper limit of the integral is less than the lower limit given this prescription, then $H(x)$ is set to unity.] Since $x = B^2 2^j = B^2 n_j$, the value of the upper limit is $x_\mathrm{max} = B^2 n(t)$.

The $G(t)$ obtained from both of these procedures is dependent on the specific form chosen for $g(t)$. This is in contrast to the calculation of N_e and G_N, which is independent of the specific time dependence of the monomer dynamics. To gain some insight into the qualitative behavior of the $G(t)$ provided by these procedures, calculations are discussed in the next section which employ the form[4,5] $g(t) = t^{1/2}$ for $t < t_\mathrm{c}$ and $g(t) = t_\mathrm{c}^{1/2}(t/t_\mathrm{c})^{2/7}$ for $t_\mathrm{c} < t < t_\mathrm{f}$ for the monomer mean-squared displacement, where t_c is the time for the crossover from unentangled to entangled dynamics and t_f is the terminal time. Since negligible relaxation is expected on long length scales, the time dependent preplateau relaxation is only influenced significantly by the chain dynamics on short and moderate length scales. Computer simulations[6,7] indicate that $g(t)$ has a behavior at short and moderate times close to the $g(t) \sim t^{1/2}$ followed by $g(t) \sim t^{2/7} \approx t^{0.28}$ dependence. If we were to employ a $g(t) \sim t^{1/2}$ followed by $g(t) \sim t^{1/4}$ dependence, as predicted by the reptation model,[3] in our calculations, the preplateau relaxation would change very little.

The time dependent relaxation of the free energy considered in the previous paragraph only accounts for the relaxation due to the motions of *entangled* chain segments on different length scales. It does not account for the total relaxation on all length scales that occurs when the chains disengage. This chain disengagement relaxation mechanism is incorporated in the calculations by multiplying the time dependent free energy expression discussed above by an additional decay factor, $F_\mathrm{d}(t)$. We use the form for $F_\mathrm{d}(t)$, which we have employed in previous work on the postplateau relaxation,[8]

$$F_\mathrm{d}(t) = \sum_{p=1,3,5,\ldots} \frac{8}{p^2\pi^2} \exp[-p^2(t/t_\mathrm{f})^{4/7} - 2^{-3/4} t/t_\mathrm{f}] \tag{7}$$

III. Calculations

In obtaining the scaling expression, eq 6, the summations in eqs 2 and 3 have been converted to integrations. To test the accuracy of this approximation, results for $N_\mathrm{e} = \Delta A_1/\Delta a$ are compared in Table 1 for the case where eq 6 is used to evaluate N_e and for the case where eqs 2 and 3 are employed. In the latter case, $f_j = (C/n_{\mathrm{ch}j})^2$ and $n_{\mathrm{ch}j} = 2^{j/2}\rho(bb_1)^{3/2}$ are used in the calculation. A value of $C = 16.1$ is employed, which is chosen on the basis of a least-squaresd fit of the predicted N_e values to the measured values. When the scaling relationship, eq 6, is employed, the proportionality

Table 1. Comparison of Experimental and Calculated Entanglement Chain Lengths

polymer[a]	b (Å)	b_1 (Å)	ρ[e]	m_0	N_e(exp)	N_e[b]	N_e[c]	N_e[d]
PE	1.54	11.364	0.0337	14.0	59.14	58.93	58.96	58.92
PEB-2	1.54	11.471	0.0324	14.6	66.85	62.15	62.17	62.13
PEB-4.6	1.54	11.425	0.0310	15.3	74.44	68.55	68.58	68.53
PEO	1.49	7.942	0.0436	14.7	110.48	114.10	114.14	114.06
PEB-7.1	1.54	10.909	0.0297	16.0	87.38	85.90	85.94	85.88
PEB-9.5	1.54	11.386	0.0285	16.7	92.93	81.89	81.92	81.87
PEB-10.6	1.54	11.701	0.0281	17.0	98.47	77.99	78.02	77.97
1,4-PBd	1.49	7.937	0.0368	13.5	134.44	159.97	160.04	159.93
PEB-11.7	1.54	10.695	0.0276	17.3	104.91	105.52	105.57	105.50
alt-PEP	1.54	9.477	0.0272	17.5	130.51	156.34	156.40	156.30
PEB-17.6	1.54	11.205	0.0254	18.9	128.73	108.41	108.45	108.38
PEB-24.6	1.54	10.844	0.0230	20.9	156.75	145.54	145.59	145.50
alt-PEB	1.54	9.436	0.0229	21.0	201.24	222.40	222.49	222.34
HHPP	1.54	9.423	0.0232	21.0	203.76	217.89	217.97	217.83
a-PP	1.54	9.136	0.0227	21.0	220.14	250.64	250.74	250.58
PEB-32	1.54	10.305	0.0210	23.0	222.78	203.81	203.89	203.76
1,4-PI	1.49	7.131	0.0294	17.0	319.35	346.43	346.56	346.33
PIB	1.54	10.401	0.0182	28.1	259.36	264.06	264.17	263.99
PMMA	1.54	13.799	0.0136	50.0	200.26	202.10	202.18	202.04
PEB-39.3	1.54	10.471	0.0194	25.0	294.84	227.85	227.94	227.79
PEB-40.9	1.54	10.001	0.0190	25.5	300.08	272.03	272.13	271.95
H_2-3,4-PI	1.54	19.271	0.0087	56.1	180.29	181.78	181.85	181.73
PS	1.54	14.655	0.0112	52.0	255.94	248.16	248.26	248.09
PDMS	1.64	10.310	0.0146	37.0	332.24	350.15	350.29	350.06
PEE	1.54	8.889	0.0180	27.0	410.52	432.24	432.41	432.12
PVCH	1.54	11.577	0.0101	55.1	707.19	630.26	630.50	630.09

[a] Polymer abreviations are the same as in Fetters et al.[3] PEB-x = poly(ethylene-*co*-butene), where x is the number of C_2H_5 side chains per 100 backbone carbons. 1,4-PBd = 1,4-polybutadiene (~50/40/10 tans/cis/vinyl). 1,4-PI = 1,4-polyisoprene (~75/20/5 cis/trans/3,4). alt-PEP = hydrogenated 1,4-polyisoprene. alt-PEB = hydrogenated 1,4-poly(ethylbutadiene) (~75/20/5 cis/trans/3,4). HHPP = head-to-head polypropylene. a-PP = atactic polypropylene. PIB = polyisobutylene. PMMA = poly(methyl methacrylate) (~75% syndiotactic). H_2-3,4-PI = copolymer of poly(isopropylethylene) and poly(1-methyl-1-ethylethylene) 75/25. PEE = poly(ethylethylene). PVCH = poly(vinylcyclohexane). [b] N_e calculated from scaling relationship, eq 6. [c] N_e calculated from eqs 2 and 3 using $f_j = (C/n_{chj})^2$. [d] N_e calculated from eqs 2 and 3 using $F_j = 1/[1 + (C/n_{chj})^2]$. [e] The density ρ is given in terms of bonds along the chain backbone per Å^3.

constant is also chosen on the basis of a least-squared fit to the experimental values for N_e. The polymer systems examined are those considered by Fetters Lohse, Richter, Witten, and Zirkel[2] (FLRWZ) at 413 K, and the values of ρ and b_1 employed in our calculations are evaluated from the FLRWZ data for the mass density and the mean-squared chain end-to-end distance divided by chain molecular weight.[2] The monomer length, b, in the table is the average bond length along the chain backbone, ρ is the number density of bonds along the backbone, and m_0 is the average chain mass per bond along the backbone. The results from the two calculations of N_e are almost identical, demonstrating that the approximations employed in obtaining the scaling relationship expressed in eq 6 are very accurate. The f_j employed has a long length scale form that agrees with the form predicted by the model calculation in Appendix B. Calculations are also presented in Table 1, which employ $F_j = [1 + (C/n_{chj})^2]^{-1}$ with $n_{chj} = 2^{j/2}\rho(bb_1)^{3/2}$ and $C = 18.95$. This form for F_j is also consistent with the long length scale dependence of F_j predicted by the model in Appendix B. The agreement between this third set of N_e values and the other two is excellent, suggesting that the value of N_e is not strongly dependent on the precise form of F_j. The root-mean-squared relative difference between the calculated and experimental values of N_e is 0.108 for each of the three calculations of N_e.

The quantities F_j, H_j, and H_j/n_j are plotted in Figure 1. The PE values of ρ, b, and b_1 at $T = 413$ K are employed, and F_j is taken to have the form $F_j = [1 + (C/n_{chj})^2]^{-1}$. The H_j values, which incorporate the effect of longer length scale relaxation on the free energy for the jth length scale, are much smaller for small j than the F_j values, which do not include this effect. The H_j and the H_j/n_j values are nearly zero for small j. The

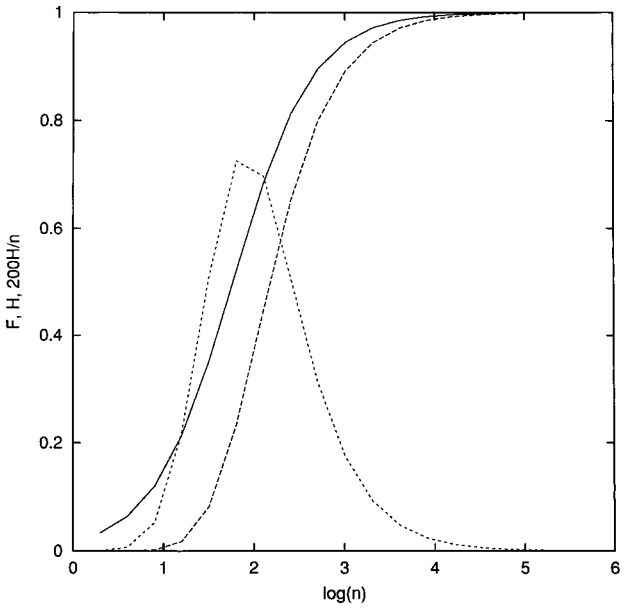

Figure 1. F_j, H_j, and $200H_j/n_j$ are plotted vs log 10(n_j). $F_j = [1 + (C/n_{chj})^2]^{-1}$ is employed with $C = 18.95$ and $n_{chj} = 2^{j/2}\rho(bb_1)^{3/2}$. Monomer parameters for PE are employed. The solid line is F_j, the dashed line is H_j, and the dotted line is $200H_j/n_j$.

figure also shows that H_j approaches unity for large n_{chj}, indicating little relaxation on longer length scales, as expected. The range of n over which H_j changes from being almost totally relaxed to almost completely unrelaxed is moderately broad, covering about an order of magnitude in n.

Figure 2 shows the calculated relaxation modulus, $G(t)$, based on the relaxation of the free energy. The results of four different calculations are presented. One

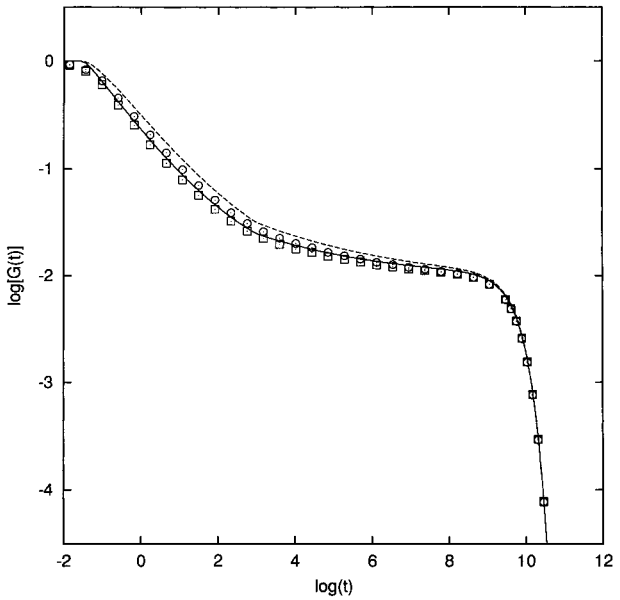

Figure 2. A log−log plot of $G(t)$ vs time. The solid curve uses $F_{j\infty} = \exp(-\alpha/n_j)$ with $\alpha = 100$ and the continuous length scale method for evaluating the relaxation. The dashed curve uses $F_{j\infty} = (1 + \alpha/n_j)^{-1}$ with $\alpha = 161.18$ and the continuous length scale method. The squares use $F_{j\infty} = \exp(-\alpha/n_j)$ with $\alpha = 72$ and associates a decay time with each discrete length scale. The circles use $F_{j\infty} = (1 + \alpha/n_j)^{-1}$ with $\alpha = 100$ and associates a decay time with each discrete length scale. The values of α are chosen so as to obtain a plateau modulus of 0.01 in all calculations.

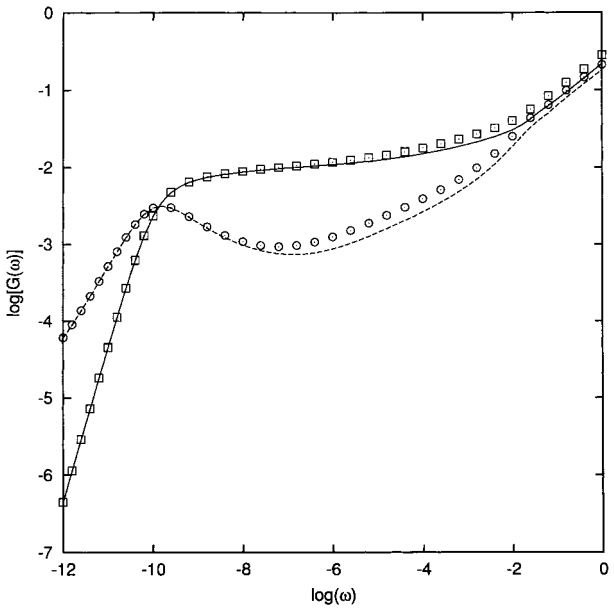

Figure 3. A log−log plot of storage and loss moduli, $G'(\omega)$ and $G''(\omega)$, vs ω. The solid curve and the dashed curve are $G'(\omega)$ and $G''(\omega)$, respectively, using $F_{j\infty} = \exp(-\alpha/n_j)$ with $\alpha = 100$. The squares and the circles give $G'(\omega)$ and $G''(\omega)$, respectively, using $F_{j\infty} = (1 + \alpha/n_j)^{-1}$ with $\alpha = 161.18$. The continuous length scale method for evaluating the relaxation is employed in all calculations.

calculation employs $F_{j\infty} = \exp(-\alpha/n_j)$ for the postrelaxation value of F_j, while the second calculation employs $F_{j\infty} = (1 + \alpha/n_j)^{-1}$. These two calculations evaluate $G(t)$ by associating a relaxation time with each length scale, as described in section II. The remaining two calculations of $G(t)$ use these same two forms for $F_{j\infty}$ but employ the continuous length scale form of the free energy, eq 4. This is also described in section II. These calculations employ a specific form for the monomer mean-squared displacement, $g(t)$. If a different form were employed for $g(t)$, the quantitative results could change some. However, simulations and most models give a $g(t)$ which is close to that employed here at short and moderate times. Therefore, we would not expect the change in the preplateau relaxation to be very large. Values of $t_c = 100$, $t_f = 10^{10}$, and $bb_1 = 1$ are used in the calculations. There is little difference between the discrete and continuous methods for associating a time dependent relaxation with the length scale dependent free energy relaxation. This is especially true when $F_{j\infty} = \exp(-\alpha/n_j)$ is employed. The initial decay has a roughly $t^{-1/2}$ dependence, although this relaxation is slightly slower when $F_{j\infty} = (1 + \alpha/n_j)^{-1}$ is used. At $t = t_c$, the relaxation crosses over to a slower decay toward the plateau value, reflecting the slowing down of the dynamics in the entangled regime. The terminal decay, which results from the disengagement of the chains and is accounted for by $F_d(t)$, eq 7, is evident around $t = t_f$ and later. The storage and loss moduli[9] are presented in Figure 3 for the two forms of $F_{j\infty}$. The results for $G'(\omega)$ and $G''(\omega)$ are evaluated from the $G(t)$ calculations using the continuous length scale form of the free energy relaxation equations. The results show that the relaxation predicted by the length scale dependent theory presented in this work is in qualitative agreement with that observed in polymer melts.

IV. Discussion

The free energy analysis presented in this work extends and improves our earlier model[1] for the length scale dependent relaxation in polymer melts. The previous work assumed a restricted form for the length scale dependent free energy, while the model presented here is more general. The analysis in this paper also accounts for the significant effect that relaxation on one length scale has on the relaxation on shorter length scales. Because this feature is neglected in the previous model, that model produces a different scaling for N_e than the current model, when an n_j dependence of n_{chj} is employed that is consistent with the model calculations in the appendices. The previous model predicts[1] $N_e \sim \rho^{-2}b_1^{-3}b^{-3}/\ln[C\rho^{-2}b_1^{-3}b^{-3}]$ where C is a constant, while the model considered in this work yields $N_e \sim \rho^{-2}b_1^{-3}b^{-3}$. While the fact that N_e is only a function of the dimensionless quantity $\rho^2b^3b_1^3$ results because the residual free energy on each length scale can depend only on n_{chj} given the model employed for the chains, the difference in the dependence of N_e on $\rho^2b^3b_1^3$ arises because the results obtained for N_e and G_N are determined by how rapidly the summations in eqs 2 and 3 converge, as well as by the n_j dependence of n_{chj}.

As can be seen from the comparison of F_j and H_j in Figure 1, the additional relaxation on shorter length scales, due to the relaxation on longer length scales, leads to significantly more relaxation on short length scales than is the case when this feature is neglected. This aspect of the analysis would affect the result for any property that is sensitive to relaxation on short length scales. The additional subsequent relaxation of the free energy for a length scale, due to the relaxation of a longer length scale, occurs on the longer time scale associated with that longer length scale. Thus, the time dependence for any process, which is sensitive to local relaxations, would also be altered by the inclusion of this feature. The development of expressions, eqs 2 and

3, for the extent of relaxation as a function of length scale is the main result of this work.

The dependence of the relaxation factors, F_j and H_j, on n_{chj} in the current analysis arises because the rescaled chain segments on each length scale have the form of harmonically bonded three-bead segments. This leaves n_{chj} as the only length scale dependent function on which F_j and H_j can depend. If the chains were not rescaled or the rescaling were accompanied by a renormalization of the interaction between segments, then these relaxation factors could also have a dependence on the number of binary contacts per chain segment on each length scale.

The calculated results for $G(t)$, $G'(\omega)$, and $G''(\omega)$ presented in section III show that the two methods employed for the evaluation of the time dependent relaxation using our length scale dependent theory provide very similar results. One of these methods associates a decay time, t_j, with the n_j for each length scale. The contribution to the excess free energy for this length scale decays exponentially with this decay time. The second method uses the continuous length scale form of the free energy expression. It considers the excess free energy to have its postrelaxation value on all length scales up to a time dependent maximum length scale for relaxation, $n(t)$, whereas length scales longer than this $n(t)$ are unrelaxed. The calculated values for $G(t)$ using these two methods are very similar. On the other hand, $G(t)$ does vary somewhat at early times depending on the n_{chj} dependence of the form employed for the relaxation factor, $F_{j\infty}$.

The plateau modulus, G_N, and the corresponding entanglement chain length, N_e, are determined by a combination thermodynamic considerations (i.e., free energy minimization) and the model employed for the length scale dependence of the free energy, which involves topological considerations, in the theory developed in this work. They are independent of the mechanism of the chain dynamics, and they are not affected by the crossover in the dynamics from Rouse-like motion to entangled motion. On the other hand, the crossover in the dynamics is apparent in the calculated modulus $G(t)$ in Figure 2 as a slowing of the initial $t^{-1/2}$ decay in the modulus. In fact, the experimental relaxation modulus has been successfully modeled[10,11] as a fast Rouse-like decay, followed by a slower decay to the plateau region, followed by the terminal relaxation at longer times. This is just what is seen in Figure 2.

In a separate series of papers,[4,5,12−14] we have presented a theory for the dynamics of polymer melts that allows for both lateral motion and motion along the chain backbones. This theory provides a scaling[12−14] for the dynamical crossover chain length, $N_d \sim b_1^3/b\sigma^2$, where σ is the average van der Waals interaction diameter for the monomer unit. This dynamical crossover chain length determines both the crossover from unentangled to entangled behavior in the time dependence of the monomer mean-squared displacement and the crossover from short to long chain behavior in the molecular weight dependence of the diffusion constant in this theory. The scaling for the crossover chain length for the dynamics, N_d, differs from the scaling predicted in this work for the entanglement length associated with the plateau modulus, $N_e \sim \rho^{-2}b^{-3}b_1^{-3}$. While both N_e and N_d result from the non-crossability of the chains, they are determined by different aspects of the polymer system. The scaling of N_e is determined in this work by the dependence of n_{ch}, the number of chain segments which are in mutual contact, on the length of the segments n, while N_d is identified in the theory for the chain dynamics with the segment length at which a pair of nearby chain segments have enough contacts so that their lateral motion relative to each other is restricted by these contacts.[12−14]

Table 2. Comparison of Experimental and Calculated Values of N_e and N_d[a]

polymer	N_e(exp)	N_e(calc)	σ (Å)	N_d
PE	59.14	58.96	3.85	600.5
PEO	110.5	114.1	3.70	229.4
PDMS	332.2	350.3	4.57	298.8
PS	255.9	248.3	9.55	209.3

[a] Also given are the values employed for the monomer interaction diameter σ in the calculation of the crossover chain length for diffusion $N_d = 9.34(b_1^3/b\sigma^2)$.

Values for the monomer interaction diameter σ have been obtained for polyethylene (PE), poly(ethylene oxide) (PEO), poly(dimethylsiloxane) (PDMS), and polystyrene (PS) from force field parameters and force field simulations.[12−14] The proportionality constant in the N_d expression has been obtained[12,13] by comparison with simulation data.[6,7] When the force field values for σ are employed, the expression for N_d has been shown to provide molecular weight dependent diffusion constants,[12−14] which are in very good agreement with experimental diffusion constant data.[15,16] The N_e obtained in this work and the previously obtained N_d values are compared in Table 2. The N_e and N_d values are significantly different. The N_e values are in good agreement with experimental data from the plateau modulus,[17] and the N_d values are in good agreement with the experimental data on the diffusion constant crossover.[12−14] However, we have only considered the N_d values for the four systems for which values of the monomer interaction diameter have been evaluated from force field parameters and force field calculations.[12−14] This is a small sample, and more work is needed in order to understand whether the N_d scaling expression holds more generally. Monomer diameters are sometimes estimated from the monomer density or crystallographic data.[18,19] However, diameters calculated in this way included free volume contributions. Furthermore, they do not always agree that well with each other or with the diameters obtained from force field parameters and simulations. For this reason, we have restricted our comparison to the cases where the force field estimates of σ are available.

The entanglement chain length associated with the plateau modulus is also not the same as the crossover chain length for the viscosity, N_c, as has been discussed recently by Fetters, Lohse, Milner, and Graessley (FLMG).[20] The viscosity is given by the time integral of the modulus, $G(t)$.[3] This integral can be broken into a contribution from the preplateau relaxation, η_1, and a postplateau contribution η_2. The postplateau contribution should be proportional to the product of the plateau modulus and the terminal relaxation time; i.e., $\eta_2 \approx G_N\tau$. The terminal time τ depends on N_d, as well as having a strong dependence on N. The dependence of τ on N_d arises because the chains move as unentangled chains longer if N_d is larger, and this results in a smaller τ. The crossover from the long chain N dependence to the short chain N dependence in the viscosity occurs when η_1 and η_2 are of comparable size, because the N dependence of the viscosity is no longer dominated by the N dependence of $\eta_2 \approx G_N\tau \sim \tau/N_e$ when N is less

than this crossover N_c. Since $\eta_2 \sim \tau/N_e$ depends on N and N_d through τ, as well as on N_e, we would expect the crossover value N_c to depend on both N_d and N_e. Thus, N_e and N_c should not be the same, in qualitative agreement with the observation of FLMG.[20] However, FLMG[20] note an empirical correlation between N_c/N_e and the packing length, $p = (\rho b b_1)^{-1}$, and it is not apparent how this simple correlation could be obtained on the basis of the scaling expressions used for N_d and N_e here. This is a point that requires further study.

As noted above, the scaling that we obtain for the N_e is the same as obtained previously by Fetters et al.[2] based on a packing length argument. Other scaling results have been obtained for N_e and N_c by various groups.[20−31] The analyses that led to these different scaling results generally begin by assuming that the entanglement molecular weight M_e or the crossover molecular weight M_c is determined by either the number of chains that can pack[2,20,24−26] into the volume spanned by a chain, R_g^3, by the number of binary contacts between pairs of chain segments,[28,29] or by the number of binary contacts in the volume spanned by a chain segment of length N_e.[30] The basis of the model for the length scale dependent relaxation presented in this work is similar to the first of these concepts. On the other hand, the N_d for the crossover in the monomer mean-squared displacement to entangled behavior in our previous work[12−14] is determined by the number of contacts between pairs of chain segments, which is the same idea as employed in the second of the concepts. We do not review the different approaches here, since they have been recently reviewed by Fetters and coworkers[2] and by Heymans.[32] Heymans[32] has suggested that the differences between some of the scaling results can be reconciled by noting an empirical correlation between the characteristic ratio for the chain, $C_\infty = b_1/b$, and the monomer aspect ratio, $a_0 = b/\sigma$.

The current analysis has discussed only linear chains. However, the free energy based argument employed here should, in principle, apply to other chain architectures as well. The important quantity in the analysis is n_{chj}, the number of segments in contact with any given segment on each length scale. The analysis of the scaling of this quantity uses the dependence of the radius of gyration on the length of the segment. In the case of branched polymers, this n_{chj} could depend on the proximity of the segment to branch points, and this would complicate the analysis. In the case of rings, computer simulations[33] indicate that the chain radius of gyration has a sightly weaker dependence on chain length, as compared with linear chains. If we take $R_g \sim n^{3/7}(bb_1)^{1/2}$ for n-monomer segments in rings, which is close to the dependence of R_g on chain length reported in recent ring simulations,[33] the argument in section II yields $n_{chj} \sim n^{2/7}\rho(bb_1)^{3/2}$ for rings, compared with $n_{chj} \sim n^{1/2}\rho(bb_1)^{3/2}$ for linear chains. If this dependence is employed and the same analysis is carried out as was performed for linear chains, then the same scaling for N_e and G_N is obtained for rings as for linear chains with a slightly different numerical prefactor. However, the extent of relaxation on each length scale is different in rings and linear chains, with a somewhat broader crossover in rings from nearly complete relaxation on short length scales to negligible relaxation on longer length scales. This discussion has only been concerned with free energy considerations. If the change in topology from linear chains to rings has a significant effect on the dynamics, then this could result in a significant change in the time dependence of the chain dynamics and relaxation. This would be reflected in quantities like the diffusion constant, the terminal time, and the viscosity, although the experimental data[34−36] do not, overall, seem to support a dramatic change in these quantities.

The chain structure is rescaled in our analysis by combining two beads on one length scale to form a single bead on the next length scale. The relaxation of a chain segment on a given length scale is treated as the relaxation of a single rescaled bead, with the two beads to which it is bonded held fixed. During this relaxation, the rescaled bead is interacting with the rescaled beads of the n_{ch} other chain segments with which its chain segment is in contact. The constraint that the chain segments cannot cross is enforced in the model calculations in the appendices through the condition that, if the x coordinate of the moving bead of one chain segment is initially less than the x coordinate for the moving bead of another chain segment, it must remain so at all later times. This amounts to using a hard-core interaction for the nonbonded bead−bead interaction on all length scales. A better rescaling procedure would also renormalize the interaction between the chains. This is a feature of the problem that we hope to consider in future work.

Acknowledgment. This has been supported by NSF Grant CHE-9816040.

Appendix A

A simple model for the relaxation of two entangled chains on a short length scale is considered. Each chain has three beads. The positions of the two end beads are held fixed, and the middle bead is allow to relax. The model is one-dimensional to simplify the handling of the constraint that the chains cannot cross. The middle bead of each chain is harmonically coupled to the end beads, so that the potential energy of this system is given by

$$V(x_a,x_b;x_{a0},x_{b0}) = k(x_a - x_{a0})^2 + k(x_b - x_{b0})^2 \quad \text{(A1)}$$

where the subscripts a and b refer to the two chains, x_a and x_b are the positions of the middle beads for the two chains, x_{a0} is the average of the positions of the two end beads for chain a, and x_{b0} is the average of the positions of the two end beads for chain b. The lack of a factor of $^1/_2$ in each harmonic term in eq A1 results because x_a and x_b are each harmonically coupled to both end beads in their chain with force constant k. It is assumed that $x_{a0} > x_{b0}$ and that $x_{0av} = (x_{a0} + x_{b0})/2 = 0$ without loss of generality. Since $x_{0av} = 0$, the dependence on x_{a0} and x_{b0} is actually a dependence only on the single variable $x_0 = x_{a0} - x_{b0}$. The constraint that the two chains cannot cross is enforced by requiring that, if $x_a > x_b$ before the application of a strain, then $x_a > x_b$ at all times after the strain. Likewise, if $x_a < x_b$ before the strain, then $x_a < x_b$ after the strain. The two cases, $x_a > x_b$ and $x_a < x_b$, are considered two different states of the system.

The system is assumed to be in equilibrium before the strain. Therefore, the probability of the system being in state 1, corresponding to $x_a > x_b$, is given by $P_1 = Q_1(x_0;\alpha)/Q(x_0;\alpha)$, and the probability of being in state 2, with $x_a < x_b$, is given by $P_2 = Q_2(x_0;\alpha)/Q(x_0;\alpha)$, where

$$Q_i(x_0;\alpha) = \int_{R_i} dx_b\, dx_a \exp[-\beta V(x_a,x_b;x_{a0},x_{b0})] \quad \text{(A2)}$$

$Q = Q_1 + Q_2$, and $\alpha = \beta k$. R_i in eq A2 is the range of allowed values for x_a and x_b. If $i = 1$, all $x_a > x_b$ are allowed, while all $x_a < x_b$ are allowed if $i = 2$.

Assuming that the system undergoes an affine deformation when the strain is applied, each coordinate, x_a, x_b, x_{a0}, and x_{b0}, is deformed to γ times its value before the strain. The probability of observing the configuration of the system, $\{x_a,x_b\}$, immediately after the strain, but before any relaxation, is proportional to its value before the strain, $\exp[-\beta V(x_a/\gamma,x_b/\gamma;\ x_{a0},x_{b0})]$, where $\{x_a/\gamma,x_b/\gamma\}$ is the prestrain configuration of the system corresponding to the poststrain configuration $\{x_a,x_b\}$. Since the strain moves all of the beads, the end bead coordinates after the strain, $\{x_{a0\gamma},x_{b0\gamma}\}$, are just γ times their value before the strain. As the system relaxes, the poststrain end bead coordinates remain fixed, while the middle beads move. The state probabilities, P_1 and P_2, are not affected by the strain or the subsequent relaxation, reflecting the noncrossability of the chains. However, the distribution of configurations within each state relaxes back to a Boltzmann distribution $\exp[-\beta V(x_a,x_b;\ x_{a0\gamma},x_{b0\gamma})]$. Thus, the distribution of configurations for the two states after the strain, but before relaxation, is given by

$$\rho_{i1}(x_a,x_b) = P_i \exp[-\beta V(x_a/\gamma,x_b/\gamma;\ x_{a0},x_{b0})][\gamma^2 Q_i(x_0;\alpha)] \quad \text{(A3)}$$

for $i = 1, 2$, with the constraint that $x_a > x_b$ for state 1 and $x_a < x_b$ for state 2. The value of the distribution is zero, if the constraint is not satisfied. The γ^2 factor is present in the denominator of eq A3 because the normalizing partition function after the strain is its value before the strain multiplied by a factor of γ for each coordinate, x_a and x_b. After the relaxation is complete, the distribution of configurations for the two states is given by

$$\rho_{i2}(x_a,x_b) = P_i \exp[-\beta V(x_a,x_b;\ x_{a0\gamma},x_{b0\gamma})]/Q_i(x_{0\gamma};\ \alpha) \quad \text{(A4)}$$

where $x_{0\gamma} = x_{a0\gamma} - x_{b0\gamma}$.

The Q_i can be readily evaluated by changing coordinates from x_a and x_b to $x_{av} = (x_a + x_b)/2$ and $x = \Delta x - x_0$, where $\Delta x = x_a - x_b$. This gives

$$Q_i(x_{0\gamma};\alpha) = \left(\frac{\pi}{2\alpha}\right)^{1/2} \int_{\mp x_0}^{\infty} dx \exp(-\alpha x^2/2) \quad \text{(A5)}$$

after the integration over x_{av} has been performed. The minus sign in the integration limit of eq A5 is used for $i = 1$, and the plus sign is used for $i = 2$. The remaining integration can be performed to give $Q_i(x_0;\alpha) = (\pi/\alpha)[1 \pm \mathrm{erf}(z_0)]$, where $z_0 = (\alpha/2)^{1/2}|x_0|$, and the plus sign is used for $i = 1$ and the minus sign for $i = 2$. The free energy of the system can be evaluated from $A = \langle E\rangle - TS$. $\langle E\rangle$ and S are given by $\langle E\rangle = \int dx_{av} \int dx\ [\rho_1 V + \rho_2 V]$ and $S = -K_B \int dx_{av} \int dx\ [\rho_1 \ln(\rho_1) + \rho_2 \ln(\rho_2)]$. The x_{av} and x integrations are both taken from $-\infty$ to ∞ with the constraint that ρ_1 is zero if $x < x_0$ and ρ_2 is zero if $x > x_0$. Since $P_i = Q_i(x_0;\alpha)/Q$ and $Q = Q_1 + Q_2 = \pi/\alpha$, the free energy for the system before the application of the strain is given by $A_0 = -K_B T \ln(\pi/\alpha)$. Immediately after the application of the strain, before relaxation has taken place, the free energy has the value

$$A_1 = A_0 + (\gamma^2 - 1)K_B T - K_B T \ln(\gamma^2) \approx A_0 + (\gamma - 1)^2 K_B T \quad \text{(A6)}$$

where the $(\gamma^2 - 1)K_B T$ term is due to the change in $\langle E\rangle$, and the $-K_B T \ln(\gamma^2)$ term comes from the extra γ^2 factor in the denominator in eq A3.

After our model system has completely relaxed subject to the constraint that the strained value for x_0 (i.e., γx_0) is held fixed, the free energy is given by

$$A_2 = A_0 + \frac{K_B T}{Q}\left(Q_1(x_0;\alpha) \ln\left[\frac{Q_1(x_0;\alpha)}{Q_1(\gamma x_0;\alpha)}\right] + Q_2(x_0;\alpha) \ln\left[\frac{Q_2(x_0;\alpha)}{Q_2(\gamma x_0;\alpha)}\right]\right) \quad \text{(A7)}$$

where $A_0 = -K_B T \ln Q$. In obtaining eq A7, $P_i = Q_i(x_0;\alpha)/Q$ and eq A4 for $\rho_{i2}(x_a,x_b)$ have been employed. Since we are interested in only the linear viscoelastic regime, we can expand A_2 about $\gamma = 1$. The zeroth-order term is just A_0, and the first-order term is readily shown to be proportional to the derivative of $Q_1(\gamma x_0;\alpha) + Q_2(\gamma x_0;\alpha) = Q$ with respect to γ, which is zero since Q is independent of γ. Thus, $A_2 \approx A_0 + (\partial^2 A_2/\partial\gamma^2)(\gamma - 1)^2/2$, and the second derivative of A_2 has the form

$$\left(\frac{\partial^2 A_2}{\partial\gamma^2}\right)_{\gamma=1} = K_B T\left[P_1\left(\frac{1}{Q_1}\frac{\partial Q_1}{\partial\gamma}\right)^2 + P_2\left(\frac{1}{Q_2}\frac{\partial Q_2}{\partial\gamma}\right)^2 - \frac{P_1}{Q_1}\frac{\partial^2 Q_1}{\partial\gamma^2} - \frac{P_2}{Q_2}\frac{\partial^2 Q_2}{\partial\gamma^2}\right]_{\gamma=1} = \frac{K_B T}{Q}\left[\frac{1}{Q_1}\left(\frac{\partial Q_1}{\partial\gamma}\right)_{\gamma=1}^2 + \frac{1}{Q_2}\left(\frac{\partial Q_2}{\partial\gamma}\right)_{\gamma=1}^2\right] \quad \text{(A8)}$$

where the γ derivatives of $Q_1(\gamma x_0;\alpha)$ and $Q_2(\gamma x_0;\alpha)$ can be obtained from eq A5.

It is worth noting that, to lowest order in $(\gamma - 1)$, $A - A_0$ is proportional to $(\gamma - 1)^2$ before and after relaxation. The value of A before relaxation, eq A6, is independent of the value of x_0, but the value after relaxation, which is obtained from eq A8, depends on x_0. The average excess free energy per segment in a melt is obtained by averaging the excess free energy over all segments in the melt, which corresponds to averaging over the distribution of x_0 values. An idea of the extent of relaxation that might be expected can be obtained by averaging eq A8 over the distribution $f(x_0) = (3\alpha/2\pi)^{1/2} \exp(-3\alpha x_0^2/2)$. This distribution corresponds to $\langle x_0^2\rangle = K_B T/3k_2$ with $k_2 = k/2$. This $\langle x_0^2\rangle$ is twice the squared radius of gyration of a chain segment on this length scale. This yields an average value of $A_2 - A_0$ of $0.0573(\gamma - 1)^2 K_B T$. Thus, there is almost, but not quite, complete relaxation in this two interacting chain model.

Appendix B

The model for chain relaxation considered in this appendix, like the one in Appendix A, is one-dimensional to simplify the treatment of the noncrossability constraints. In this case, there are many other chain segments constraining the motion of a selected chain segment. The selected chain segment is referred to as chain A. The starting point for this model is $A = \langle E\rangle - T\langle S\rangle = \sum_j [\int \rho_j V\ dx + K_B T \int \rho_j \ln \rho_j\ dx]$. In the previous model, there are two possible regions or states: $x_a < x_b$

and $x_a > x_b$. In the current model, we allow many states for chain A. Each state is characterized by an x_{Li} and an x_{Ui}, the lower and upper allowed values for x_a, where x_a is the position of the middle bead in a three-bead segment representing chain A on a given length scale. Thus, the starting equation for this model is

$$A_j(\lambda) = K_B T \sum_i P_i[\ln(P_i) + \int_{R_{ij}} dx\, f_{ij}(x)(\ln[f_{ij}(x)] + \beta V(x))] \quad \text{(B1)}$$

where $j = 0$ before the strain, $j = 1$ after the strain but before relaxation, and $j = 2$ after the relaxation is complete. P_i in eq B1 is the probability of being in state i in the equilibrium system, and R_{ij} is the range of allowed values of x for state i, which goes from x_{Li} to x_{Ui} when $j = 0$ and from γx_{Li} to γx_{Ui} when $j = 1$ or $j = 2$. The distribution of configurations for state i is given by $\rho_{ij}(x) = P_i f_{ij}(x)$, if x is in the allowed range for state i, and it is zero otherwise. After the strain but before relaxation, $f_{i1}(x) = {D_{i1}}^{-1} \exp[-\beta V(x/\gamma)]$, which is proportional to the Boltzmann weight for the prestrain coordinate x/γ corresponding to the poststrain coordinate x. After the relaxation, the distribution is given by the Boltzmann distribution, $f_{i2}(x) = {D_{i2}}^{-1} \exp[-\beta V(x)]$, where the D_{ij} are determined by the condition that the integral of $f_{ij}(x)$ over R_{ij} is unity.

The various states of the system correspond to different positionings of chain A relative to the surrounding chains. For example, the upper limit of the integration region, R_{ij}, results from the noncrossability constraint between chain A and a surrounding chain segment with which it makes contact at this point. Another integration region results, if chain A is placed on the other side of this chain. The system is then in a different state, and what was the upper integration limit for the old state is now the lower limit of the integration region for the new state. In defining the states of the system for the evaluation of the free energy of chain A, we consider only the states obtained by allowing chain A to cross the backbones of the surrounding states. There is no need to consider the states produced by allowing two of the surrounding chain segments to cross each other.

In this model, x_{Li} and x_{Ui} are treated as fixed objects. The poststrain chain motions should allow the surrounding chains, as well as chain A, to move and relax. The use of fixed objects to model the constraints simplifies the analysis considerably. The averaging of the motions of the surrounding chains, subject to the constraints of noncrossability and no relaxation on longer length scales, produces a potential of mean force for the motion of chain A. The use of fixed barriers to the motion of chain A is equivalent to approximating the potential of mean force as a hard wall box potential. This model corresponds to the evaluating the relaxation of each chain holding the configurations of all others fixed. The range of motion of chain A for a fixed configuration of the surrounding chains is obviously much less than would be the case if the surrounding chains were allowed to move. Although this fixed-surrounding-chain procedure does not capture all of the relaxation, it is assumed that it provides a reasonable estimate of the magnitude of the relaxation in the free energy.

The one-dimensional model considered here is intended to mimic real three-dimensional systems. In a three-dimensional system, chain A may bump into one chain if it moves in one direction and bump into a different chain if it moves in a different direction. It can also occur that the motion of chain A in a specific direction would cause it to contact one chain for some configurations of the surrounding chains but cause it to contact a different chain for other configurations. Placing chain A on the opposite side of these different chains correspond to different states of the system, as long as these new configurations cannot be reached from one another without crossing a chain backbone. The summation over different states in the equations for the model should apply equally well for the one-dimensional and three-dimensional cases. However, in the three-dimensional case, some reasonable mathematical prescription would have to be found to enforce the noncrossability constraints and to keep the motions of a chain segment from allowing it to go around the ends of other segments.

If the regions R_{ij} are small, which corresponds to a large number of other chain segments in contact with chain A, then $f_{ij}(x)$ is well approximated by expanding the potential around x_{ij}, the midpoint of R_{ij}. If the $\exp[-\beta V(x_{ij})]$ factor is absorbed into D_{ij}, this expansion yields

$$f_{ij}(x) = {D_{ij}}^{-1} \exp\left(-\beta\left[V'_{ij}(x - x_{ij}) + \frac{1}{2}V''_{ij}(x - x_{ij})^2\right]\right) \quad \text{(B2)}$$

with the definitions $V_{i0}(x) = V_{i2}(x) = V(x)$ and $V_{i1}(x) = V(x/\gamma)$. If f_{ij} from eq B2 is substituted into eq B1, and f_{ij} and V are expanded to quadratic order in $x - x_{ij}$, and if a quadratic expansion is also used in the evaluation of D_{ij}, then A_j takes the form

$$A_j = K_B T \left\langle \sum_i P_i \left(\ln\left[\frac{P_i}{\gamma \Delta_i}\right] + V_{i2} + \frac{\gamma^2 \beta}{24}[V''_{i2} + \beta V'_{ij}(V'_{ij} - 2V'_{i2})]{\Delta_i}^2 \right) \right\rangle \quad \text{(B3)}$$

where $\Delta_i = x_{Ui} - x_{Li}$ and $\langle ... \rangle$ indicates an average over all configurations of the constraining chains. Using the fact that $V'_{i1} = V'_{i2}/\gamma$, eq B3 gives

$$\Delta A_1 - \Delta A_2 = \langle \sum_i P_i \gamma^2 \beta (V'_{i1} - V'_{i2})^2 {\Delta_i}^2/24 \rangle$$
$$= (\gamma - 1)^2 \langle \sum_i P_i \beta V'(x_{i0})^2 {\Delta_i}^2/24 \rangle \quad \text{(B4)}$$

for the difference in the poststrain excess free energy before and after the relaxation, to the lowest order in $\gamma - 1$. As the number of other chain segments in contact with chain A increases, the range of x for the different states decreases proportionately, so that $\Delta_{i1} \sim 1/n_{ch}$. Thus, the decrease in the excess free energy upon relaxation scales as $\Delta A_1 - \Delta A_2 \sim 1/{n_{ch}}^2$. (The number of states in the summation over i increases as n_{ch} increases, but the probabilities decrease proportionally, so that $\sum_i P_i$ remains unity. Thus, these two feature should cancel when determining the n_{ch} dependence of $\Delta A_1 - \Delta A_2$.)

If this one-dimensional model is generalized to the three-dimensional case, each expansion point x_i is replaced by a vector $\mathbf{r}_i$, which is chosen such that the integral of $\mathbf{r} - \mathbf{r}_i$ over the region R_{ij} vanishes. The free energy expression becomes the sum of x, y, and z terms,

each having the form given by eqs B3 and B4. If the strain is an elongation, the γ in eq B4 is equal to γ for the direction of the elongation, while it is $\gamma^{-1/2}$ for the other two directions. If α equals x, y, or z, then the derivatives V' and V'' are replaced by corresponding α derivatives, V_α and $V_{\alpha\alpha}$, respectively, and Δ_{ij}^2 is replaced by the average of $4(\alpha - \alpha_i)^2$ over R_{ij} for each term in the summation over the x, y, and z coordinates. The cross terms [which contain $(\alpha - \alpha_i)(\lambda - \lambda_i)$, where α and λ are each x, y, or z but are not the same] vanish due to the configurational averaging in the free energy expressions. As in the one-dimensional case, the quantities $\langle(\alpha - \alpha_i)^2\rangle_{ij} \sim 1/n_{ch}^2$. Thus, $\Delta A_1 - \Delta A_2 \sim 1/n_{ch}^2$ should also hold for a three-dimensional generalization of this model.

References and Notes

(1) Herman, M. F.; Panajotova, B. V. *Comput. Theor. Polym. Sci.* **1997**, *7*, 101.
(2) Fetters, L. J.; Lohse, D. J.; Richter, D.; Witten, T. A.; Zirkel, A. *Macromolecules* **1994**, *27*, 4639.
(3) Doi, M.; Edwards, S. F. *The Theory of Polymer Dynamics*; Clarendon: Oxford, 1986.
(4) Herman, M. F.; Panajotova, B.; Lorenz, K. T. *J. Chem. Phys.* **1996**, *105*, 1153.
(5) Herman, M. F.; Panajotova, B.; Lorenz, K. T. *J. Chem. Phys.* **1996**, *105*, 1162.
(6) Kremer, K.; Grest, G. S. *J. Chem. Phys.* **1990**, *92*, 5057.
(7) Paul, W.; Binder, K.; Heermann, D. W.; Kremer, K. *J. Chem. Phys.* **1991**, *95*, 7726.
(8) Tong, P.; Herman, M. F. *J. Chem. Phys.* **1995**, *102*, 7700.
(9) Ferry, J. D. *Viscoelastic Properties of Polymers*; Wiley: New York, 1980.
(10) Lodge, T. P.; Rotstein, N. A.; Prager, S. *Adv. Chem. Phys.* **1990**, *79* 1.
(11) Lin, Y.-H. *Macromolecues* **1984**, *17*, 2846; **1986**, *19*, 159, 169.
(12) Panajotova, B. V.; Herman, M. F. *J. Chem. Phys.* **1998**, *108*, 5122.
(13) Herman, M. F.; Panajotova, B. V. *J. Chem. Phys.* **1999**, *110*, 8792.
(14) Panajotova, B. V.; Herman, M. F. *Macromolecules* **2000**, *33*, 3932.
(15) Pearson, D. S.; Ver Strate, G.; von Meerwall, E.; Schilling, F. C. *Macromolecules* **1987**, *20*, 1133.
(16) Fleischer, G. *Colloid Polym. Sci.* **1987**, *265*, 89.
(17) The experimental PE values for the plateau modulus and entanglement molecular weight in Fetters et al.[2] are obtained by extrapolating the PEB-x data to $x = 0$, where PEB-x is poly(ethylene-*co*-butene) and x is the number of $-C_2H_5$ side chains per 100 backbone carbon atoms.
(18) Zang, Y.-H.; Carreau, P. J. *J. Appl. Polym. Sci.* **1991**, *42*, 1965.
(19) He, T.; Porter, R. S. *Makromol. Chem., Theor. Simul.* **1992**, *1*, 119.
(20) Fetters, L. J.; Lohse, D. J.; Milner, S. T.; Graessley, W. W. *Macromolecules* **1999**, *32*, 6847.
(21) Graessley, W. W.; Edwards, S. F. *Polymer* **1981**, *22*, 1329.
(22) Aharoni, S. M. *Macromolecules* **1983**, *16*, 1722.
(23) Ronca, G. *J. Chem. Phys.* **1983**, *79*, 1031.
(24) Lin, Y. H. *Macromolecules* **1987**, *20*, 3080.
(25) Kavassalis, T. A.; Noolandi, J. *Macromolecules* **1988**, *21*, 2869.
(26) Kavassalis, T. A.; Noolandi, J. *Macromolecules* **1989**, *22*, 2709.
(27) Iwata, K.; Edwards, S. F. *J. Chem. Phys.* **1989**, *90*, 4567.
(28) de Gennes, P.-G. *J. Phys., Lett.* **1974**, *35*, L-133.
(29) Wu, S. *Polym. Eng. Sci.* **1990**, *30*, 753.
(30) Colby, R. H.; Rubinstein, M.; Viovy, J.-L. *Macromolecules* **1992**, *25*, 996.
(31) Wool, R. P. *Macromolecules* **1993**, *26*, 1564. (See ref 2 concerning errors in data in this paper.)
(32) Heymans, N. *Macromolecules* **2000**, *33*, 4226.
(33) Brown, S.; Szamel, G. *J. Chem. Phys.* **1998**, *108*, 4705.
(34) McKenna, G. B.; Hadziioannou, G.; Lutz, P.; Hild, G.; Strazielle, C.; Straupe, C.; Rempp, P.; Kovacs, A. J. *Macromolecules* **1987**, *20*, 498.
(35) Mills, P. J.; Mayer, J. W.; Kramer, E. J.; Hadziioannou, G.; Lutz, P.; Strazielle, C.; Rempp, P.; Kovacs, A. J. *Macromolecules* **1987**, *20*, 513.
(36) Tead, S. F.; Kramer, E. J.; Hadziioannou, G.; Antonietti, M.; Sillescu, H.; Lutz, P.; Strazielle, C.; Rempp, P.; Kovacs, A. *Macromolecules* **1992**, *25*, 3932.

MA001268D